

Technical University of Denmark



## Some puff modelling principles relevant for dispersion calculations in the atmosphere

Mikkelsen, Torben Krogh; Larsen, Søren Ejling; Troen, Ib

*Publication date:*  
1980

*Document Version*  
Publisher's PDF, also known as Version of record

[Link back to DTU Orbit](#)

*Citation (APA):*  
Mikkelsen, T., Larsen, S. E., & Troen, I. (1980). Some puff modelling principles relevant for dispersion calculations in the atmosphere. (Risø-M; No. 2258).

## DTU Library

Technical Information Center of Denmark

---

### General rights

Copyright and moral rights for the publications made accessible in the public portal are retained by the authors and/or other copyright owners and it is a condition of accessing publications that users recognise and abide by the legal requirements associated with these rights.

- Users may download and print one copy of any publication from the public portal for the purpose of private study or research.
- You may not further distribute the material or use it for any profit-making activity or commercial gain
- You may freely distribute the URL identifying the publication in the public portal

If you believe that this document breaches copyright please contact us providing details, and we will remove access to the work immediately and investigate your claim.

RISØ-M-2258

SOME PUFF MODELLING PRINCIPLES RELEVANT FOR DISPERSION  
CALCULATIONS IN THE ATMOSPHERE

T. Mikkelsen, S.E. Larsen and I. Troen

Abstract. Some basic principles for a computational puff-model for prediction and simulation of atmospheric dispersion are discussed. The constraints imposed by use of a single point measurement of the windfield for advection of puffs are examined. A simple scheme for simulation of a more realistic windfield is proposed. One example of the use of a puff-model is shown and comparison is made with an ordinary Gaussian plume model.

INIS descriptors: ADVECTION, BOUNDARY LAYERS, COMPUTERIZED SIMULATION, DIFFUSION, EARTH ATMOSPHERE, MATHEMATICAL MODELS, METEOROLOGY, PLUMES, TRAJECTORIES, WIND.

UDC 551.510.4 : 681.3.06

September 1980

Risø National Laboratory, DK 4000 Roskilde, Denmark

ISBN 87-550-0716-3

ISSN 0418-6435

Risø Repro 1980

---

**CONTENTS**

**Page**

<b>1. BASIC PRINCIPLES AND COMPUTATIONAL STRUCTURE .....</b>	<b>7</b>
<b>2. THEORY .....</b>	<b>12</b>
<b>2.1. The scatter of puff centers .....</b>	<b>15</b>
<b>2.2. The size and growth of the puffs .....</b>	<b>16</b>
<b>3. EXAMPLE OF THE USE OF A PUFF MODEL .....</b>	<b>19</b>
<b>4. REFERENCES .....</b>	<b>25</b>
<b>APPENDIX A: Statistical modelling of spatial and temporal variability .....</b>	<b>26</b>

---

**PREFACE**

This report is based on lecture notes, which partly formed the conduct of a speech given by N.E. Busch as lecture 17 in "Mathematical simulation of air pollution dispersion", a meeting held by "Nordic co-operative organization for applied research" in Helsinki, 2-11 September 1980, and partly formed the conduct of a workshop contribution given by T. Mikkelsen at the same occasion.



## 1. BASIC PRINCIPLES AND COMPUTATIONAL STRUCTURE

The basic principle for a computational puff-model for prediction and simulation of atmospheric dispersion can be understood qualitatively by studying Fig. 1a. Here, the figure shows an instantaneous topview contour of a smoke plume propagating in the mean wind direction from its point of release. Also shown is the contour of the average long term concentration distribution corresponding to an ordinary Gaussian plume model. The instantaneous plume is represented by means of a puff-model in which the circles represent individual puffs. The puff-model is seen to simulate the instantaneous plume picture by distribution of puffs of different sizes.

The concentration distribution in an individual puff is often hypothesised to be Gaussian in all three dimensions. The standard deviation  $\sigma_{\text{puff}}$  represents the puff size. From the lateral dispersion coefficients in Fig. 1b we see the importance of distinguishing between the instantaneous plume dispersion or the puff-size and the long term averaged distribution  $\sigma_{\text{Gauss plume}}$ .

Figure 1a also shows that a puff-model has the advantage that it makes it possible to account for the instantaneous behaviour of the plume. Where the Gaussian plume model represents a statistical time averaged concentration pattern, the puff-model is capable, in principle, to simulate an updated instantaneous plume picture by means of a corresponding actual wind field, even when this is instationary and inhomogeneous.

The computational structure of a numerical puff-model can for instance have the form suggested in the block diagram in Fig. 2.

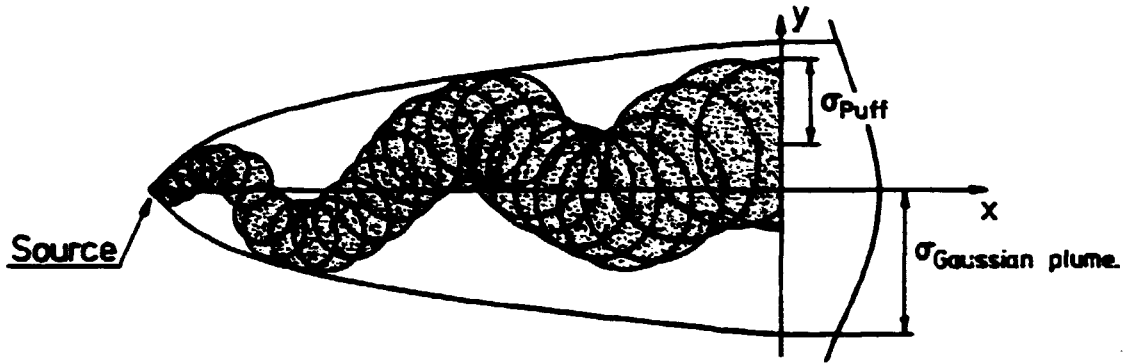


Fig. 1a. The figure illustrates the difference between the Gaussian plume model and the puff model principle. The instantaneous plume (shaded area) is well represented by the chain of puffs of different sizes whereas the Gaussian plume model represents a stationary long term average of the lateral concentration distribution, as function of downwind distance  $x$ .

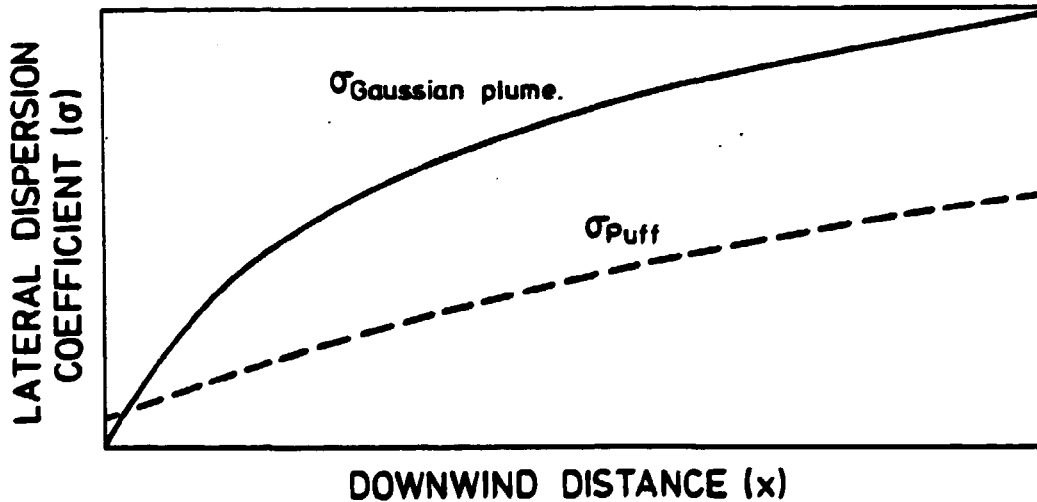


Fig. 1b. The lateral dispersion coefficient of the Gaussian plume model (full line) versus the lateral puff size from fig. 1a, as function of downwind distance.



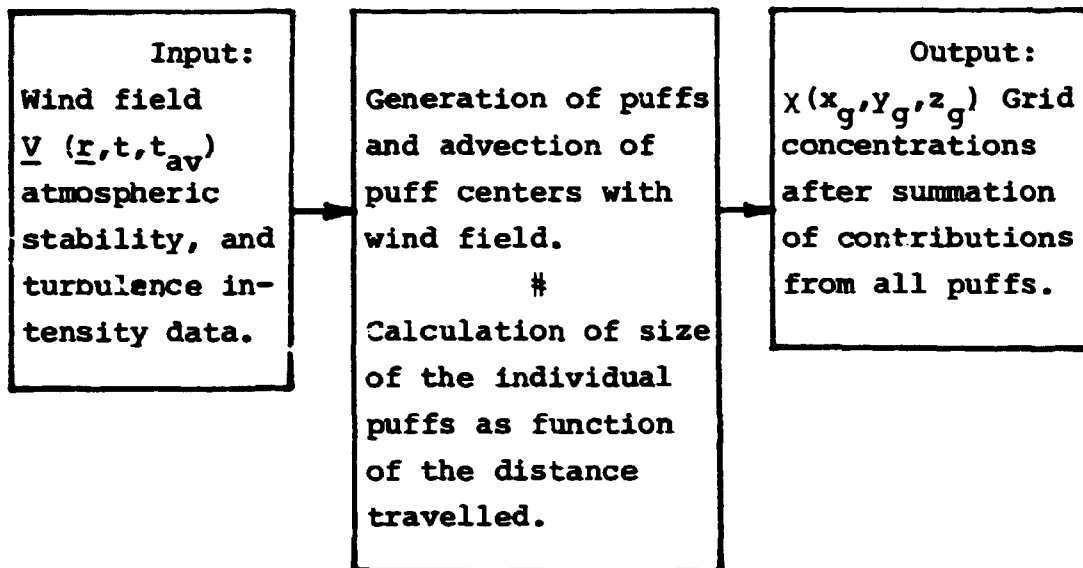


Fig. 2. Model structure

The technique suggested here is to generate puffs with specified release rates in a specified grid. The individual puffs are advected by the wind field  $\underline{V}$ , which in general is a specified function of coordinate  $\underline{r}$ , time  $t$  and averaging time  $t_{av}$ . We write

$$\underline{V} = \underline{V}(\underline{r}, t, t_{av}) \tag{1}$$

To compute the growth and buoyant lift of all the puffs it is necessary to have a simultaneous specification of the turbulence intensity and the atmospheric stability.

Once the advection and size of all puffs has been calculated, updated grid concentrations  $\chi(x_g, y_g, z_g)$  are obtained at each grid point  $(x_g, y_g, z_g)$  by summing up all the contributions from the puffs in the grid.

Assuming Gaussian distributions and total ground reflection the formula for the concentration in grid point  $(g)$  from puff number  $(i)$  is given by:

$$\chi_i(x_g, y_g, z_g) = \frac{Q(i)}{(2\pi)^{3/2} \sigma_p(i) \sigma_z(i)} \exp\left[-\frac{1}{2}\left(\frac{x_g - x_c(i)}{\sigma_p(i)}\right)^2 + \left(\frac{y_g - y_c(i)}{\sigma_p(i)}\right)^2\right] \times \quad (2)$$

$$\left[ \exp\left(-\frac{1}{2}\left(\frac{z_g - z_c(i)}{\sigma_z(i)}\right)^2\right) + \exp\left(-\frac{1}{2}\left(\frac{z_g + z_c(i)}{\sigma_z(i)}\right)^2\right) \right]$$

where

- $Q(i)$  : Release fraction in puff no. (i) (unit mass), which in turn is given by: (Release rate from the source [mass/time]) × (elapsed time between puff-release [time]).
- $x_c(i), y_c(i), z_c(i)$  : Centre coordinates of puff no. (i).
- $\sigma_p(i), \sigma_z(i)$  : Puff-sizes in horizontal and vertical plane, respectively.

In dealing with microscale and with mesoscale puff models, the wind field  $\underline{v}$  in eq. (1) should be obtained by an "objective" wind field analysis, based on simultaneous measurements of wind speed and direction from a network of meteorological towers, positioned over the area of interest for the dispersion calculation. One way to come around this complication, however, is to base the implementation scheme on wind data from a single point, thereby making the input data easier obtainable. Utilization of one point measurements for describing the dispersion of airborne material at distances far from the point of measurement, however, requires an extreme high degree of coherence over the distances of interest. In the atmosphere, the shortest time scale,  $\Delta T$ , on which coherence can be expected between a measurement point and a downwind distance  $D$ , is typically one

order of magnitude larger than the time a puff uses to move from its release at the measurement point to D. Running a puff-model on the basis of wind vectors averaged over such long time intervals would result in a quasistationary concentration distribution featuring no improvements relative to the application of an ordinary Gaussian plume model.

Therefore, if it for convenience is decided to run a puff-model on the basis of wind measurements at a single point only, averages must be taken over much shorter time intervals than  $\Delta T$ , but then one has to accept the fact that an instantaneous puff picture computed in this way is comparable to the real plume only in the following sense:

A puff-model, using a single point measurement of the wind field, advects puffs by means of the recorded wind field at the measurement point, and thus it does not include the spatial variability inherent in the true wind field. For the special situation where the total dispersion is essentially contributed to from the centre of mass fluctuations and the relative diffusion of the puffs plays only an insignificant part, the standard deviation  $\sigma(t)$  of the distribution function can be estimated by:  $\left(2\overline{v'^2} t_E t\right)^{\frac{1}{2}}$  in the far field limit where  $t \gg t_E$ .

$\overline{v'^2}$  is the variance of the lateral wind component and  $t_E$  is the Eulerian integral time scale. The true spread in the atmosphere can on the other hand be estimated by the same expression, but with the Eulerian time scale  $t_E$  replaced by the Lagrangian time scale  $t_L$ . So, still in the far field limit, the dispersion calculated by a puff model using a single point measured wind-field, will predictably be underestimated by a factor of the order  $\sqrt{\beta}$ , where  $\beta$  is the ratio between the Lagrangian and Eulerian integral time scales.

Each puff's trajectory, which is explicitly modelled by the advection scheme can then be perceived as one realisation of the single particle trajectory calculation, which by time averaging generates the downwind distribution function as the case is in absolute diffusion.

Further, it should be pointed out that the application of single point measurements as input to a model limits its validity to situations in which the turbulence can be assumed to be horizontal homogenous. Consequently, it is important to make sure that the record of single point measurements used in a simulation is representative for the properties of turbulence for the domain in question.

Alternative ways to simulate the true, but often inaccessible wind field  $\underline{V}(\underline{r},t)$  may be suggested. Investigations of a 1. order autoregressive computational scheme seems promising for the simulation of both the spatial and temporal variability of a dispersing wind field. Such a auto-regressive scheme requires as input data only one recorded time serie of the dispersing wind field, together with an estimate of the spatial correlation length scale. See appendix A for a further discussion.

## 2. THEORY

Let us first derive an important result by which diffusion in an absolute frame of reference in a puff-model, can be related to the diffusion in the relative frame attached to the centre of gravity of a puff, the so called relative diffusion.

Consider the release at time = 0 of a puff into a field of stationary and homogeneous turbulence. Let the observed concentration field at subsequent times in an individual realization of the experiment be  $\chi(\underline{x},t)$ . This field is subject to the continuity equation, which in integral form reads

$$Q = \int \chi(\underline{x},t) d\underline{x} \quad (3)$$

where  $Q$  is the total amount of matter released with the puff. The volume integral extends over all space. The components of the position vection  $\underline{x}$  will be designated  $(x_1, x_2, x_3)$  so that

$d\underline{x}$  is the volume element  $dx_1 dx_2 dx_3$ .

The first moment of the concentration field  $\chi(\underline{x}, t)$  yields the position vector  $\underline{c}$  of the center of gravity

$$\underline{c} = \frac{1}{Q} \int \underline{x} \chi(\underline{x}, t) d\underline{x} \quad (4)$$

For an individual realization  $\underline{c}$  is a random function of time.

A relative position vector may now be defined by

$$\underline{y} = \underline{x} - \underline{c} \quad (5)$$

with components  $(y_1, y_2, y_3)$ .

The observed concentration field may also be described in the "relative" frame of reference, the center of which,  $\underline{c}(t)$  moves about in a random manner. We have clearly  $\chi(\underline{y}, t) = \chi(\underline{x} - \underline{c}, t)$ . This only differs from the "fixed" frame description in the trivial point of a different coordinate origin. Significant differences exist, however, between the statistical properties of  $\chi$  as observed at a fixed  $\underline{x}$  and fixed  $\underline{y}$ , respectively.

The zeroth and first moment of the concentration distribution in the  $\underline{y}$ -frame are clearly

$$\int \chi(\underline{y}, t) d\underline{y} = Q \quad (6)$$

$$\int \underline{y} \chi(\underline{y}, t) d\underline{y} = 0 \quad (7)$$

For the second moment of the instantaneous concentration distribution in the  $\underline{x}$  and  $\underline{y}$  frames we have, by use of the definition of a center of gravity, eq. (4)

$$\begin{aligned}
 & \int y_i y_j \chi(\underline{y}, t) d\underline{y} & (8) \\
 & = \int (x_i - c_i) (x_j - c_j) \chi(\underline{x}, t) d\underline{x} \\
 & = \int x_i x_j \chi(\underline{x}, t) d\underline{x} + c_i c_j \int \chi(\underline{x}, t) d\underline{x} \\
 & \quad - c_i \int x_j \chi(\underline{x}, t) d\underline{x} - c_j \int x_i \chi(\underline{x}, t) d\underline{x} \\
 & = \int x_i x_j \chi(\underline{x}, t) d\underline{x} - c_i c_j Q.
 \end{aligned}$$

for any  $i$  and  $j$  ( $= 1, 2$  or  $3$ ).

As explained in the introduction, it is the statistical properties of the diffusion process which concern us, specially the ensemble-mean field at fixed  $\underline{y}$ ,  $\langle \chi(\underline{y}, t) \rangle$ . Therefore, to characterize second moments of ensemble average quantities, we define the following mean square dispersion tensors

$$\Sigma_{ij} = \frac{1}{Q} \int x_i x_j \langle \chi(\underline{x}, t) \rangle d\underline{x} \quad (9)$$

$$\delta_{ij} = \frac{1}{Q} \int y_i y_j \langle \chi(\underline{y}, t) \rangle d\underline{y} \quad (10)$$

$$m_{ij} = \langle c_i c_j \rangle \quad (11)$$

From eq. (8) we have then, after ensemble-averaging:

$$\Sigma_{ij} = \delta_{ij} + m_{ij} \quad (12)$$

To exhibit the physical meaning of this last relation a little more clearly, consider a specific component of the dispersion tensors involved, say  $i = j = 2$ , and write

$$\begin{aligned}\sigma_{y,abs}^2 &= \Sigma_{22} \\ \sigma_{y,rel}^2 &= S_{22} \\ \sigma_{y,c.m.}^2 &= M_{22}\end{aligned}\tag{13}$$

so that  $\sigma_{y,abs}$ ,  $\sigma_{y,puff}$  and  $\sigma_{y,c.m.}$  are the lateral length scales (standard deviations) of their respective distributions. We may call  $\sigma_{y,abs}$  standard deviation of the "absolute" dispersion,  $\sigma_{y,rel}$  that of "relative" or puff diffusion and  $\sigma_{y,c.m.}$  that of "center of mass" or "meandering". Equation (12) shows then that

$$\sigma_{i,abs}^2 = \sigma_{i,rel}^2 + \sigma_{i,c.m.}^2\tag{14}$$

In other words, absolute dispersion is the sum of relative dispersion and meandering, in the sense that their variances are additive. Clearly,  $\sigma_{i,abs}$  is always greater than either  $\sigma_{i,rel}$  or  $\sigma_{i,c.m.}$ .

We have shown that the diffusion calculation in a puff model can be concentrated on the two different variables  $\sigma_{i,c.m.}$  and  $\sigma_{i,rel}$  and we will continue the development by separate considerations about the contributions to the total plume width from each.

### 2.1. The scatter of puff centers, $\sigma_{i,c.m.}$

The scatter of a puff's center position is explicitly modelled by the advective wind field, eq. (1) and should not, in principle, concern us further, because the mechanism in the advection scheme automatically will determinate that. In a more sophisticated puff-model, however, the velocity used for the advection of the individual puffs should be calculated on the basis of the expression

$$\frac{dc}{dt} = \frac{1}{Q} \int V(\underline{x}, t) \cdot \chi(\underline{x}, t) dx \quad (15)$$

which defines the velocity of the "center of mass" of the puff  $\chi(\underline{x}, t)$  at time  $t$ .

## 2.2. The size and growth of the puffs, $\sigma_{i,rel}$ :

The calculation of relative diffusion or puff size for use in operationally dispersion models has for a long time been, and is still, a topic of intensive discussion and research.

A simple but obviously inconsistent approach to estimating instantaneous puff size is the use of classification schemes (Pasquill, 1974, Turner, 1967) derived from continuous releases (Gauss plumes) lasting from  $\frac{1}{2}$  to 1 hour, see e.g. the puff model by Start and Wendell, 1974. Another approach for the determination of instantaneous puff size involves overall fit to power laws of observed puff sizes. Gifford, 1977, for example, finds  $\sigma_{i,rel} \propto t^{1.2}$  as a good compromise in the troposphere for travel times over 5-6 orders of magnitude.

Though theory and modelling technique of relative diffusion is far from having been developed to the extent that is the case of absolute diffusion, its role is indeed not unimportant.

Smith and Hay (1961) derived an expression for the growth rate of a puff with an isotropic Gaussian density distribution embedded in homogeneous and isotropic turbulence.

By considering only times beyond the initial stage, i.e.  $\bar{u} t \gg \sigma_p$ , where  $\sigma_p$  is the standard deviation of the puff, their equation for the growth rate in terms of the Eulerian energy spectrum function of turbulence  $E(k)$ , becomes



$$\frac{d\sigma_p}{dt} = \frac{\pi}{3} \frac{\beta_t}{\bar{u}} \int_0^{\infty} E(k) \frac{1 - e^{-\sigma_p^2 k^2}}{\sigma_p k} dk \quad (16)$$

Here  $k$  is the wave number in radians per unit length and  $\beta_t = \frac{3}{4}\beta$ , where  $\beta$ , the ratio between the Lagrangian and Eulerian time scales, is around 4.

The weighting function  $(1 - e^{-\sigma_p^2 k^2})/\sigma_p k$  in eq. (16) is in effect a "bandpass filter", which accentuates that part of the 3-dimensional spectrum which is most effective in determining the rate of growth of a cluster.

The finite size of the cluster is taken into account by the "roll off" on the low frequency side of the weighting function. The "roll off" on the high-frequency side represents the diminishing contribution to the dispersion, as the eddy size decreases to a magnitude small compared to the dimension of the cluster, see the following figure.

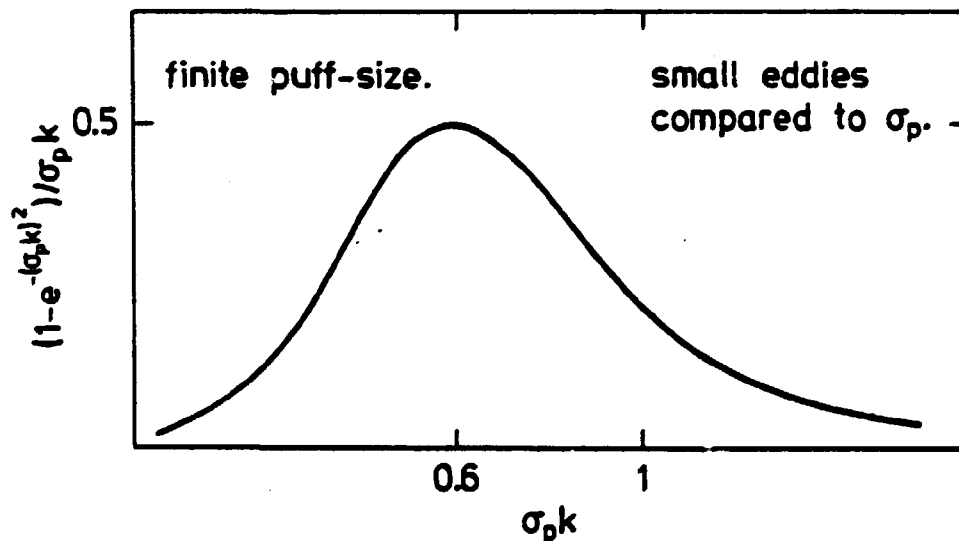


Fig. 3. The weighting function in eq. (16)

By assuming an exponential Eulerian auto-covariance function, numerical evaluation of (16) shows that the maximum value of

$d\sigma_p/dx$  is well approximated by

$$\left(\frac{d\sigma_p}{dx}\right)_{\max} = \frac{2}{3} \beta_t i^2 \quad (17)$$

where  $\underline{i}$  is the intensity of turbulence  $(u'^2)^{1/2} / \bar{u}$ .  $u'$  is the vector component of the eddy velocity. Smith and Hay show that the rate of expansion downwind is almost constant and equal to the maximum value  $(d\sigma_p/dx)_{\max}$  over a wide range of  $\sigma_p/l$ , where  $l$  is the turbulent length scale. Hence, eq. (17) constitutes a simple practical formula for evaluation  $\sigma_p$ , once an estimate of the intensity  $\underline{i}$  is given.

Pasquill (1974) suggests that the relation  $\beta_t \cdot i = 0.33$ , due to Wandel and Kofoed-Hansen (1962), should be adopted for consistency between the similarity and statistical theory of turbulence. Substitution of this  $\beta_t$  in (17) yields

$$\left(\frac{d\sigma_p}{dx}\right)_{\max} = \frac{2}{3} \beta_t \cdot i^2 = 0.22 \cdot i \quad (18)$$

Pasquill also considers the data obtained by Högström (1964) carried out under "very stable" atmospheric conditions at an intermediate downwind range (50-5000 m). He finds a discrepancy between eq. (18) and averaged data from the two sites Agesta and Studsvik of the order -27% and +11%, respectively.

The conclusion derived from the above referred analysis is that there seems to exist a good correlation between the growth of puffs and the intensity of turbulence, which is not surprising because the parameter  $\underline{i}$  itself contains information about other meteorological parameters such as surface roughness and atmospheric stability. In some atmospheric workbooks, e.g. Slade (1968),  $\underline{i}$  alone is consequently applied as a quantitative stability measure, corresponding to Pasquill A through F type of stability classes.

Since eq. (18) needs only the parameter  $\underline{i}$  as input for the determination of  $\sigma_p(x)$ , it is easily implemented in a puff model to give an estimate of puff sizes as function of distance travelled.

### 3. EXAMPLE OF THE USE OF A PUFF-MODEL TO CALCULATE DISPERSION FROM A SOURCE WITH VARIABLE TIME OF RELEASE

The following example is taken from Mikkelsen et al. (1980) in which the dispersion from a nuclear accident was analysed by the use of a puff-model.

Fig. 4 shows the development of a puff chain controlled by the wind at the source point. The time between release of puffs is 200 s, hence 3 puffs are advected with each consecutive 10 min. averaged wind vector. With the 50 puffs released, the total release duration becomes ~ 2h 47 min. The puff chain is shown 1, 3, 5 and 7 hours after a simulated release. 20 km downwind from the source, the puffs have here grown to a lateral size of the order ~ 600 m. Fig. 5 shows iso-lines of the ground level concentration dose which results from the plume passage in fig. 4.

In fig. 6 comparison is made between the Gaussian plume model and the puff model crosswind distributions at a line perpendicular to the mean wind direction ~ 20 km downwind from the source. Distributions from both models are shown for cases with constant source strength of duration equal to  $\frac{1}{2}$  hour as well as for an exponentially decaying source with time constants  $\tau$  equal to 200, 600 and 1800 seconds. Where the Gaussian plume models distribution have constant width (560 m), the crosswind dose distributions of the puff model is seen to be strongly influenced by the time dependency of the source strength. The width of the puff models dose distributions for the cases with constant source strength and  $\tau = 200$  s (700 - 800 m) are not much in excess of the lateral size of the puff ~ 600 m at the downwind distance considered. This indicates that the contribution to the distribution from the scatter in puff centres is relatively small. For the cases with  $\tau = 600$  s and  $\tau = 1800$  s, however, this effect contributes significantly to the total width. The standard deviation of the crosswind dose distribution with  $\tau = 1800$  s is approximately 3 km, ~ 5

times the width of the corresponding Gaussian plume model's distribution.

For short term releases we see that the shape of the dose distribution of the puff model and the Gaussian plume model are alike. However, the crosswind position of the distribution relative to the Gaussian plume models centreline is dependent on the average direction of the wind field in the time interval during which the puff-plume is under advection from the source to the downwind receptor position. On the other hand, when the time of release becomes longer, the puff model is in contrast to the Gaussian plume model, able to take into consideration the successive larger contribution to the total spread resulting from the relative displacement of the puffs centre position.

FIGURE LEGEND

Fig. 4. Development of a puff-plume by the wind field recorded from Risø meteorological mast at height of 117 m, starting at 11:30 p.m. on May 23 1975. The wind field is identical to case no. 2, fig. 3.2 in Risø report R-356. The puff-plume is shown top viewed 1, 3, 5 and 7 hours after start of release. Puffs are released consecutively at 200 s intervals, a total of 50 puffs are released.

Fig. 5. Ground level concentration dose resulting from the puff-plume passage in fig. 4 for the time constant for the source  $\tau$ , equal to 1800 sec. Iso-dose lines are shown for maximum dose:  $D_{\max} \text{ gsm}^{-3}/2^n$ ;  $n = 1.2, \dots 9$ . The vertical broken line corresponds to the distance from the source, where results from the puff model and a plume model is compared.

Fig. 6. Comparison of ground level crosswind dose distribution of the Gaussian plume model at  $x = 23.2$  km and the puff model at  $x = 20.0$  km (puff trajectories = 23.2 km) under conditions of identical vertical deviation,  $\sigma_z = 65$ .

Gauss model:  $\sigma_y = 560$  m,  $\sigma_z = 65.0$  m ( $x = 23.2$  km)

Puff model:  $\sigma_p \approx 600$  m,  $\sigma_z = 65.0$  m  
( $x = 20$  km, puff trajectory  $\approx 23.2$ )

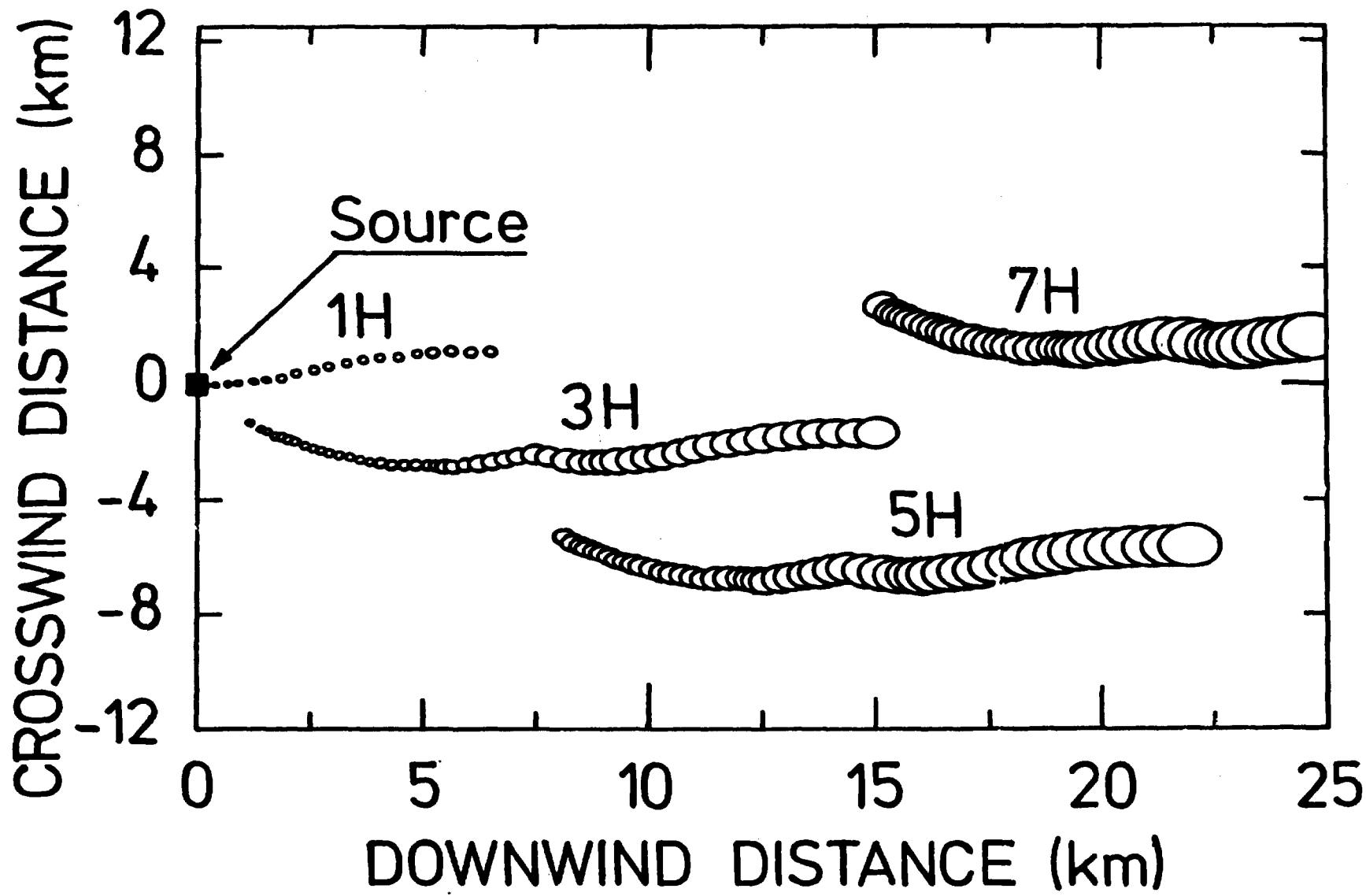


Fig. 4

Fig. 5

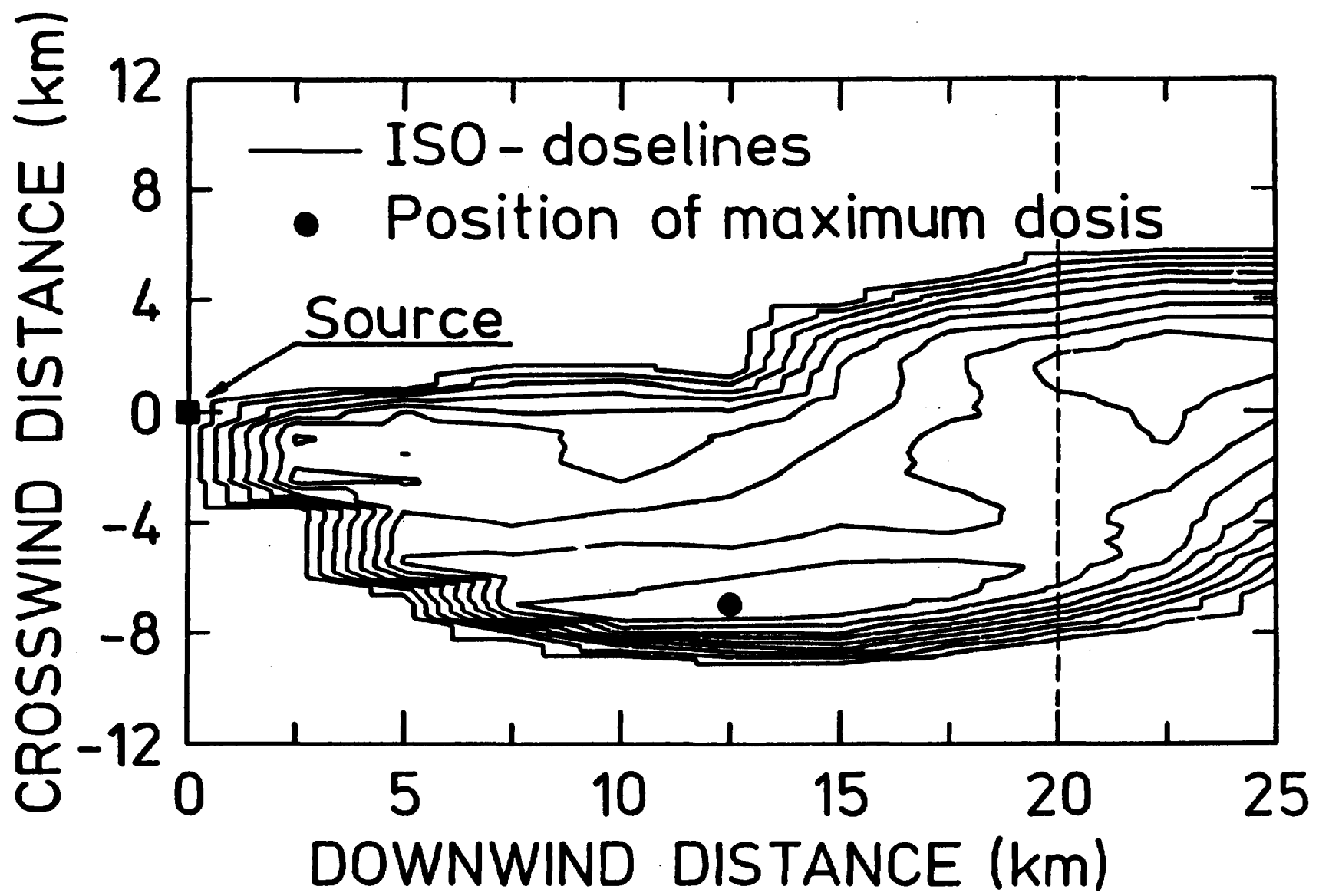
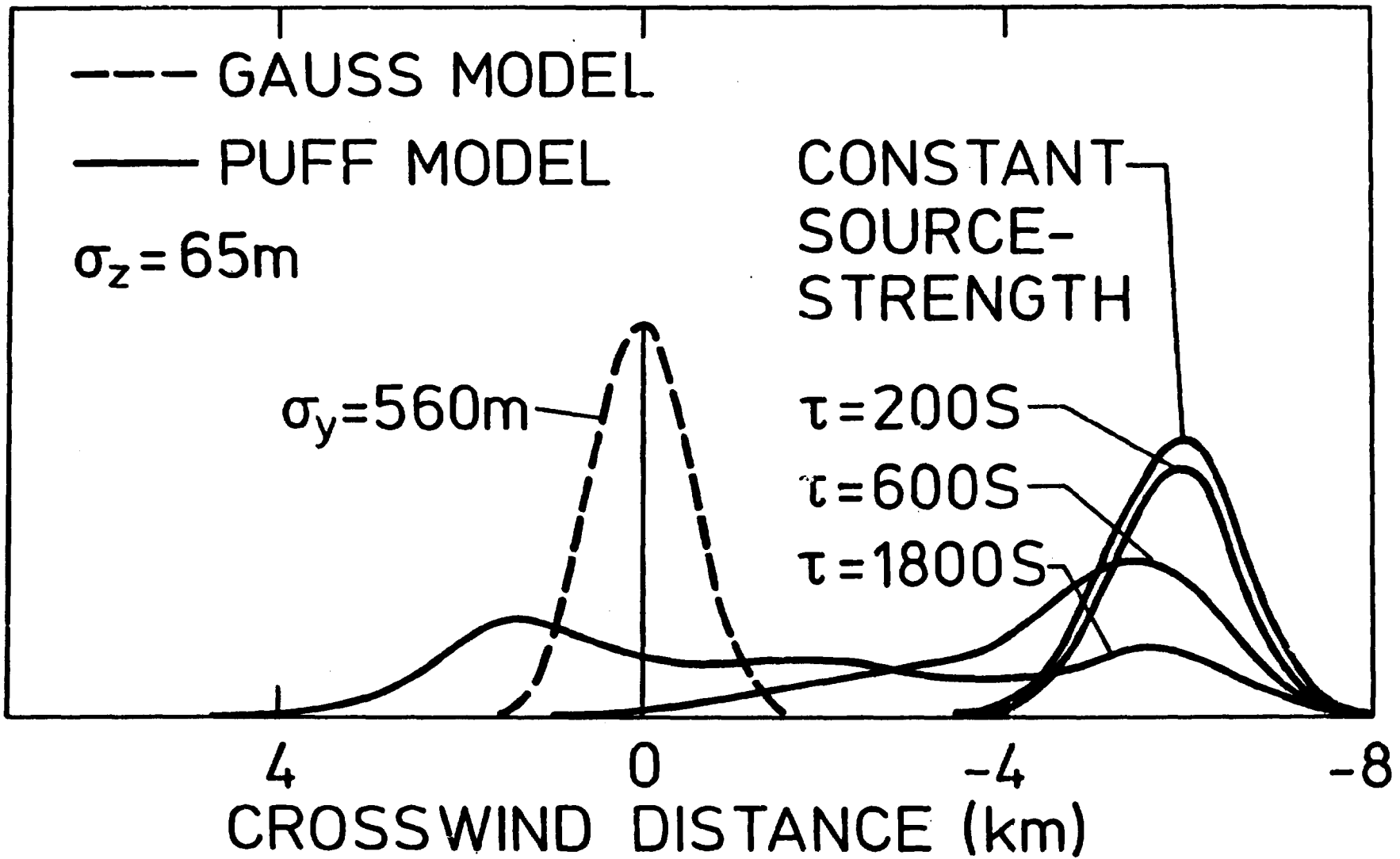


FIG. 6

CROSSWIND DISTRIBUTION





REFERENCES

- GIFFORD, F.A., Tropospheric Relative Diffusion Observations, *Journal of Applied Meteorology*, 16, p. 311, 1977.
- HÖGSTRÖM, H., An experimental study on atmospheric diffusion. *Tellus* 16, p. 205, 1964.
- JENSEN, P.H., PETERSEN, E.L., THYKIER-NIELSEN, S., and VINTHER, F.H., Calculation of the Individual and Population Doses on Danish Territory Resulting from Hypothetical Core-melt Accident at the Barsebäck Reactor, Risø Report No. 356, 122 pp., 1977.
- MIKKELSEN, T., LARSEN, S.E., and TROEN, I. Use of a puff-model to calculate dispersion from a strongly time-dependent source. To appear in proceeding of the "European Seminar on Radioactive Releases and the Dispersion in the Atmosphere following a Reactor Accident", Risø, 22-25 April, 1980. The proceeding should appear in the fall 1980.
- PASQUILL, F., *Atmospheric Diffusion*, 2nd Ed., John Wiley & Sons, New York, xi + 429 pp., 1974.
- SLADE, D.H., *Meteorology and Atomic Energy*, U.S. Atomic Energy Commission, 1968.
- SMITH, F.B., and HAY, J.S., The expansion of clusters of particles in the atmosphere, *Quart. J.R. Met. Soc.*, 87, p. 82, 1961.
- START, G.E., WENDELL, L.L., Regional Effluent Dispersion Calculations considering Spatial and Temporal Meteorological Variations. NOAA Technical Memorandum ERL-ARL-44, 1974.
- TURNER, D.B., *Workbook of Atmospheric Dispersion Estimates*, Environmental Protection Agency, North Carolina, 84 pp., 1970.
- WANDEL, C.F. and KOFOED-HANSEN, O., On the Eulerian-Lagrangian transform in the statistical theory of turbulence, *J. Geophys. Res.*, 67, p. 3089, 1962.
- WENDELL, L.L., Mesoscale wind fields and transport estimates from a network of wind towers, *Mon. Wed. Review*, 100, p. 565, 1972.

APPENDIX A

Statistical Modelling of Spatial and Temporal Variability

In principle a puff-model can describe dispersion under inhomogeneous and instationary conditions, as described in the main body of the text. This ability, however, can be fully utilised only, if the wind field used for advection of the puffs are known in detail as function of space and time, within the computational grid.

Such a procedure is often neither possible nor practical. Hence the need arises for physical and statistical schemes for interpolation/extrapolation of the wind field data, which are available and on which a simulation of the dispersion can be based. Here we describe a statistical scheme, which can be used for a simulation of the spatial structure of the wind field from a measured time series at the source point.

We display first the principles of a 1. order autoregressive computational scheme, which seems promising for the simulation of spatial and temporal variability in combination, of a dispersing wind field.

$$U(t + \Delta t) = \rho_L U(t) + U^-(t + \Delta t) \quad (A1)$$

$$U^-(\text{puff no. } i+1) = \rho_0 U^-(\text{puff no. } i) + \text{white noise process} \quad (A2)$$

Two 1. order autoregressive equations are shown, the first of which (A1) governs the time development of (e.g. the lateral) velocity  $U$  of the  $i$ 'th puff on the basis of the Lagrangian correlation coefficient  $\rho_L$ .

The next 1. order autoregressive process (A2) relates the  $U$ 's of neighbouring puffs at the same time through the (Eulerian) correlation coefficient,  $\rho_0$ .

The two equations are inter-connected in that the "noise"  $U$  in the first process is taken as the spatial correlated velocities of the second process.

In fig. A1 is shown the puff plume of fig. 4, as it appears 5 hours after the start of release. This puff plume is advected as a stiff system by the single point measured wind field directly.



Fig. A1. The puff plume in fig. 4 as it appears 5 hours after the start of release.

Next, in fig. A2 is shown the corresponding puff plume that results when the single point measured wind field is fed into the auto regressive simulation model.  $\Delta t$  is 10 min here, so the puff plume at time  $(t + \Delta t)$  corresponds to the situation 5 hours 10 min after the first puff is released.

Finally, a  $\rho_L \rho_O$ -diagram is shown in fig. A3 from which the different possible regimes of operating the auto regressive model can be inferred. The point  $(\rho_L, \rho_O) = (0, 1)$  corresponds to the case in fig. A1 above. The point (x) simulated the puff plume in fig. A2. For a more detailed discussion, see Mikkelsen et al. (1980).

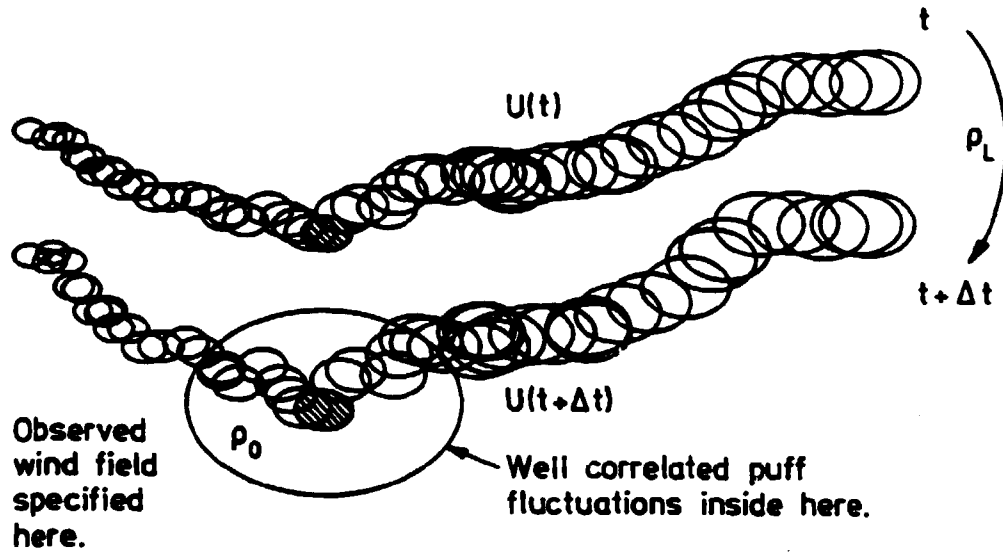


Fig. A2. The puff plume of fig. A1 as it appears, when the single point wind field is fed into the autoregressive simulation model. The plume is shown at the top at time: 5 hours after start at release, and below one advection step (10 min) later.

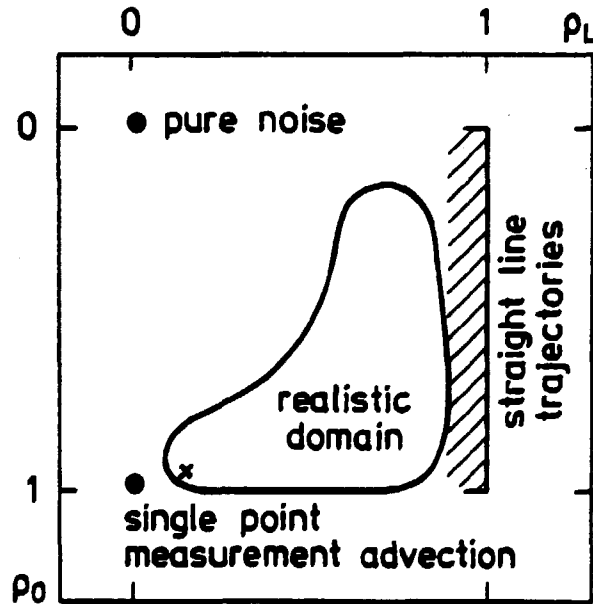


Fig. A3.  $\rho_L \rho_0$ -diagram showing the different possible regimes of operating the autoregressive model.

